STM JOURNALS

Journal of
Materials & Metallurgical Engineering

ISSN: 2231-3818 (Online)
ISSN: 2321-4236 (Print)
Volume 16, Issue 2, 2026
May–August
DOI (Journal): 10.37591/JoMME

https://journals.stmjournals.com/jomme

Research JoMME

Experimental Analysis and Optimization of Pulse TIG Welding Parameters for Dissimilar Aluminum Alloys

Sagarkumar Shah[1,*], Pratik Kikani[1], Jaydeepkumar Chavda[2]

Abstract

Tungsten inert gas (TIG) welding is highly regarded as the primary welding method, especially for challenging metals like aluminum. Pulsed-current TIG welding has been specifically developed for welding aluminum alloys. Composite weld joints of aluminum alloys AA5052 and AA6063 find extensive use in diverse sectors such as automotive and marine applications, where significant mechanical properties and corrosion resistance are required. It is crucial to carefully select the process parameters to achieve the desired mechanical and physical properties in the welded structure. The ASME Section IX provides valuable guidelines for determining the essential input parameters for TIG welding. This research project aims to investigate the influence of specific welding parameters, including peak current, base current, and pulses per second. For the composite welding of 8 mm thick plate joints of AA5052 alloy and AA6063 alloy, ER4043 filler wire is employed. Tensile tests are used to evaluate composite joints' mechanical characteristics and weld strength. The central composite design (CCD) and regression analysis are applied to identify the welding parameter that significantly affects the results. The response surface optimizer is utilized to optimize the selected parameters, and the outcome is thoroughly evaluated to meet the requirements as per ASME/ASTM standards.

Keywords: Aluminum composite alloys, AA5052 alloy, AA6063 alloy, pulsed-current TIG welding, tensile strength, hardness, response surface method.

INTRODUCTION

Aluminum (Al), a metal initially proposed by Sir Humphrey Davy in the early 1800s, was successfully isolated by Hans Christian Ørsted in 1825. However, it remained largely confined to laboratories for approximately three decades. It was not until 1886 that limited commercial production of aluminum commenced, owing to the development of a practical industrial extraction process for obtaining aluminum from bauxite, its mineral source. This extraction method was independently developed by Charles M. Hall and Paul Héroult, and their groundbreaking process is still in use today. Owing to its highly reactive nature, aluminum is not naturally found in its metallic state but exists in various forms within the Earth's crust [1].

During the early 1900s, a significant portion of aluminum was obtained from waste and scrap materials. This source alone contributes approximately 2 million tons of aluminum alloys annually in Europe, including the United Kingdom. However, the resulting pure aluminum is relatively weak and therefore not extensively used, particularly in construction applications. To increase its mechanical strength, pure aluminum is frequently alloyed with metals such as copper (Cu), manganese (Mn), magnesium (Mg), silicon (Si), and zinc (Zn) [2].

***Author for Correspondence**
Sagarkumar Shah
E-mail: sagarkumar.shah@atmiyauni.ac.in

[1]Assistant Professor, Department of Mechanical Engineering, Atmiya University, Gujarat, India
[2]P.G. Scholar, Department of Mechanical Engineering, Atmiya University, Gujarat, India

Received Date: May 22, 2026
Accepted Date: May 29, 2026
Published Date: June 22, 2026

Citation: Sagarkumar Shah, Pratik Kikani, Jaydeepkumar Chavda. Experimental Analysis and Optimization of Pulse TIG Welding Parameters for Dissimilar Aluminum Alloys. Journal of Materials & Metallurgical Engineering. 2026; 16(2): 1–12p.

Aluminum-copper alloys emerged as one of the initial alloy combinations to be developed. Around 1910, the concept of age or precipitation hardening in this alloy family was recognized, leading to its rapid adoption in the emerging field of the aviation industry. Subsequently, numerous alloys within this category have been developed, possessing strengths similar to high-quality carbon steel but at a significantly lighter weight, approximately one-third of the weight [1].

Aluminum composite alloys, such as AA5052 and AA6063, provide a blend of lightweight strength, superior corrosion resistance, and excellent thermal and electrical conductivity. They are easily machinable, providing versatility for complex applications, and exhibit enhanced weldability for strong, defect-free joints, even in dissimilar combinations [3, 4]. These materials can be customized through alloying elements to meet specific requirements, such as increased ductility, hardness, or fatigue resistance. Aluminum composite alloys are commonly used in the aerospace, automotive, marine, construction, and electronics industries. These alloys offer exceptional performance and are environmentally friendly owing to their recyclability. These alloys are indispensable in modern engineering, offering durability and adaptability across diverse applications [2].

This study emphasizes the application of pulsed-current TIG welding parameters for aluminum composite alloys. These parameters were carefully selected, investigated, and optimized through experimental work. The findings add to the present research and have significance for sustainable design and future research. Pulsed-current tungsten inert gas (TIG) welding is a modified version of traditional TIG welding that employs intermittent current pulses rather than a continuous flow [5, 6]. This strategy is widely applied in many sectors owing to its numerous advantages. When pulsed-current TIG welding is employed, the power supply alternates between high-peak and low-background currents [7]. While the background current sustains the arc, allowing cooling and solidification, the peak current produces sufficient heat to melt the base metal and create a weld pool [8]. A key advantage of pulsed-current TIG welding is its superior control over the heat input compared with that of conventional TIG welding. By adjusting pulse parameters such as the peak current, background current, pulse duration, and frequency, welders can achieve precise control over the weld bead profile, penetration depth, and heat-affected zone [9, 10]. This welding method lowers the chances of distortion and burn-through, making it particularly useful for welding thin materials or complex welds. It also facilitates improved regulation of the heat-affected zone, leading to reduced metallurgical alterations and enhanced weld quality. Moreover, pulsed-current TIG welding enables increased welding speeds while maintaining the integrity of the weld. The pulsing action enhances arc stability, regulates heat input, and provides better control over the dynamics of the weld pool. Pulsed-current TIG welding is used in numerous sectors, including aerospace, automotive, manufacturing, and precision welding. Pulsed TIG is frequently used to weld non-ferrous metals, including stainless steel and aluminum [11].

The response surface method (RSM) is a widely used statistical modeling and optimization technique applied in engineering, scientific research, and quality improvement processes [12]. Its primary purpose is to analyze and optimize complex relationships between input variables and the desired response or output variable. RSM leverages diverse statistical tools and techniques to analyze and optimize the response surface model [13]. The design of experiments (DOE) is commonly employed to efficiently sample the input variable space and generate data for model fitting. The response surface model was then examined to determine the ideal input variable settings using methods such as regression analysis, analysis of variance (ANOVA), and optimization algorithms [14]. In conclusion, the RSM is a statistical tool for modeling and optimization, aimed at analyzing and improving the relationship between input variables and the desired response variable [15].

EXPERIMENTAL WORK

Materials and Welding Process

For the experiments, AA5052 and AA6063 dissimilar plates were used, which were cut into dimensions of 100 mm × 50 mm × 8 mm. These plates served as weld coupons and were joined along the joint lines. The alloy compositions (wt.%) of the base metal and filler material were obtained from ASME Section II, as presented in Table 1 [16].

Manual welding of AA5052 and AA6063 dissimilar aluminum alloys was performed using the pulsed-current tungsten inert gas welding (PC-TIG) technique with a Miller Dynasty machine. ER4043 was employed as the welding consumable in accordance with ASME Section II, Part C [17]. The average chemical analysis of the welding consumable, expressed as a percentage by weight, is provided in Table 1. To create a butt joint, a single V-groove was prepared with a root face of 2 mm, root gap of 2 mm, and V-angle of 60°. Pulsed-current gas tungsten arc welding (GTA) was employed to join the base plates of AA5052 using ER4043 filler material. Table 2 outlines the welding parameters employed in the pulsed-current tungsten inert gas (PC-TIG) welding process. The welded specimens were subjected to liquid penetrant testing in accordance with ASME Section V [18].

Mechanical Properties

Tensile tests were conducted using a universal testing machine at room temperature. Twenty specimens were prepared following the guidelines outlined in ASTM E8M-04 to ensure consistent results. Rockwell hardness tests were conducted using a Rockwell hardness tester, following the specifications outlined in ASTM E18 [19]. The tests were performed on a Rockwell hardness scale of HRC to obtain accurate hardness measurements.

Design of Experiment

Experimental design (ED) or DOE is a crucial stage in statistical process control (SPC). This involves the utilization of different experimental designs to attain optimal results. These designs can be quantitatively represented to optimize the parameters and enhance the overall performance.

The central composite design (CCD) is a specific type of response surface design employed in studies aimed at determining the optimal values for multiple independent variables or components. The CCD incorporates three types of experimental variables: factor levels, axial points, and center points. This design was utilized to efficiently explore and analyze the relationships between variables and identify the best settings for achieving the desired outcomes. Table 3 shows the total number of experiments created in the Design-Expert software [20].

Optimization and Validation

The optimization process typically involves defining the problem, identifying the objective function, specifying the constraints, and selecting an appropriate method. Common optimization methods include gradient-based algorithms, evolutionary algorithms, linear programming, and heuristics. Optimization is the process of identifying the ideal solution or set of values for a particular objective function while meeting specific constraints or criteria. The goal can vary depending on the situation, such as increasing profit, reducing cost, or improving system performance. Optimization techniques utilize mathematical algorithms, modeling, simulation, and statistical methods to search for optimal solutions within a defined parameter space.

Table 1. Alloy chemical composition (wt.%) of AA5052, AA6063, and ER 4043 filler.

Base/filler metal	Al	Si	Fe	Mg	Cr	Mn	Zn	CU
AA5052	96.78	0.13	0.3	2.5	0.2	0.05	0.03	0.01
AA6063	93.84	5.82	0.09	<0.001	<0.001	-	<0.001	0.02
ER4043	93.84	5.82	0.09	<0.001	<0.001	-	<0.001	0.02

Table 2. Welding input parameters and their range.

Input parameters	Low	Medium	High
Peak current (Amps)	160	180	200
Base current (Amps)	80	90	100
Pulse per second (Hz)	100	130	150

Table 3. Design of experiment combination.

Exp. No.	Peak current (Amp.)	Base current (Amp.)	Pulse per second (Hz)
1	160	80	110
2	160	80	150
3	160	90	130
4	160	100	110
5	160	100	150
6	180	80	130
7	180	90	110
8	180	90	130
9	180	90	130
10	180	90	130
11	180	90	130
12	180	90	130
13	180	90	130
14	180	90	150
15	180	100	130
16	200	80	110
17	200	80	150
18	200	90	130
19	200	100	110
20	200	100	150

In contrast, validation is the process of confirming the accuracy, dependability, and efficacy of a model, system, or solution. It aims to assess whether the optimized solution meets the intended objectives and performs as expected in real-world scenarios. Validation involves comparing the results obtained from the optimized solution with empirical data, experimental observations, or established benchmarks.

Response Surface Method and Confirmation

Once the response surface model is established, it can serve several purposes. These include predicting the response for untested input variable combinations, determining the optimal settings of input variables to achieve the desired response, and performing sensitivity analyses to assess the relative significance of various variables. By constructing a response surface model and utilizing statistical analysis tools, RSM enables efficient experimentation, prediction, optimization, and improvement of processes and systems.

Confirmation of findings is a crucial part of the scientific method and the research process. The confirmation process involves conducting additional experiments or studies that aim to replicate the original findings. These replication attempts can be performed by the original or independent researchers to ensure objectivity and eliminate any biases. The confirmation process may also involve different methodologies, sample sizes, or experimental conditions to strengthen the robustness of the findings. The fundamental goal of confirmation is to evaluate the consistency and reliability of the original results. If replication studies yield similar outcomes, it provides confidence in the validity and generalizability of the initial findings. In summary, confirmation involves replicating and verifying experimental findings or results to ensure their reliability, validity, and reproducibility.

RESULT AND DISCUSSION

In this current research work, there are three input parameters and two output parameters which are involved in this current work. The results of the output responses are discussed below.

Table 4. Design of experiment with output responses.

Exp. no.	Peak current (Amps)	Base current (Amps)	Pulse per second (Hz)	Hardness (HRC)	Tensile strength (MPa)
1	160	80	110	54	133.84
2	160	80	150	56	136.08
3	160	90	130	56	140.45
4	160	100	110	56	145.10
5	160	100	150	60	157.79
6	180	80	130	62	151.43
7	180	90	110	62	157.68
8	180	90	130	63	159.11
9	180	90	130	63	148.08
10	180	90	130	64	148.67
11	180	90	130	66	158.84
12	180	90	130	68	159.11
13	180	90	130	70	158.75
14	180	90	150	72	159.73
15	180	100	130	73	173.17
16	200	80	110	77	185.96
17	200	80	150	82	169.29
18	200	90	130	85	170.63
19	200	100	110	90	202.21
20	200	100	150	94	205.10

Experimental Data Analysis

The ED was built using a CCD in Design-Expert software and a mix of data. Table 4 presents the design of the experiment with the response.

A liquid penetrant test was also performed to inspect the weld quality. The specimens were observed after the test, and they were all defect-free and accepted as per the ASME SEC. VIII DIV.1

Response Discussion

The response discussion is essential for analyzing the behavior of the output responses. In this study, two output responses were considered: hardness and tensile strength. Some 3D surface plots represent the output response analysis.

The hardness of the material exhibits a notable correlation with the peak current, as depicted in the 3D surface plot in Figure 1. The hardness increased proportionately with an increase in the peak current. Furthermore, a higher peak current resulted in a greater level of hardness.

The relationship between the peak current and hardness was striking, indicating a significant impact. Changes in the peak current strongly influenced the hardness of the material, as shown in Figure 2 (3D surface plot). It is clearly seen in the graphs that when peak current increases, hardness increases, but when pulse per second changes, it is less effective compared to peak current. A higher peak current leads to higher hardness.

A remarkable correlation between the peak current and tensile strength can be observed in the material, as illustrated in Figure 3 (3D surface plot). An increase in the peak current is directly proportional to the increase in the tensile strength. Additionally, a higher peak current resulted in a higher tensile strength.

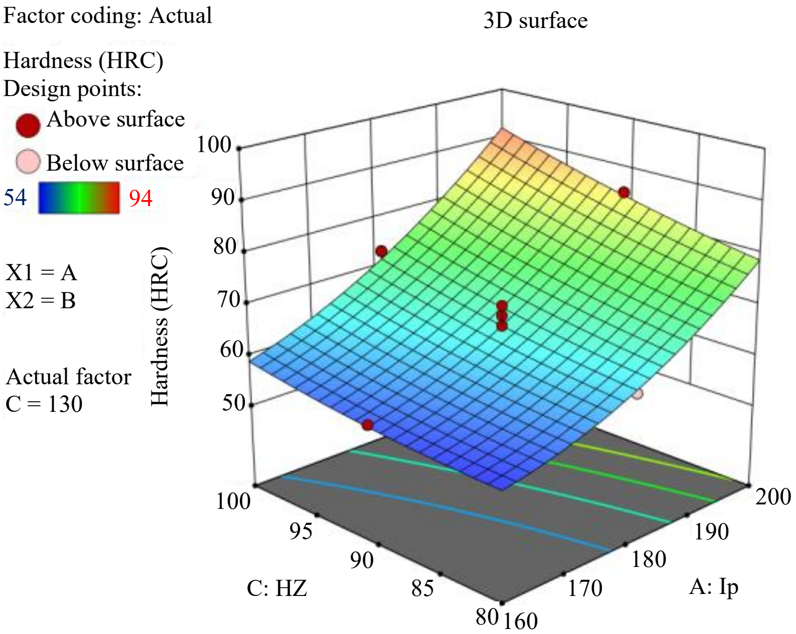

Figure 1. 3D surface plot of peak current and base current for hardness.

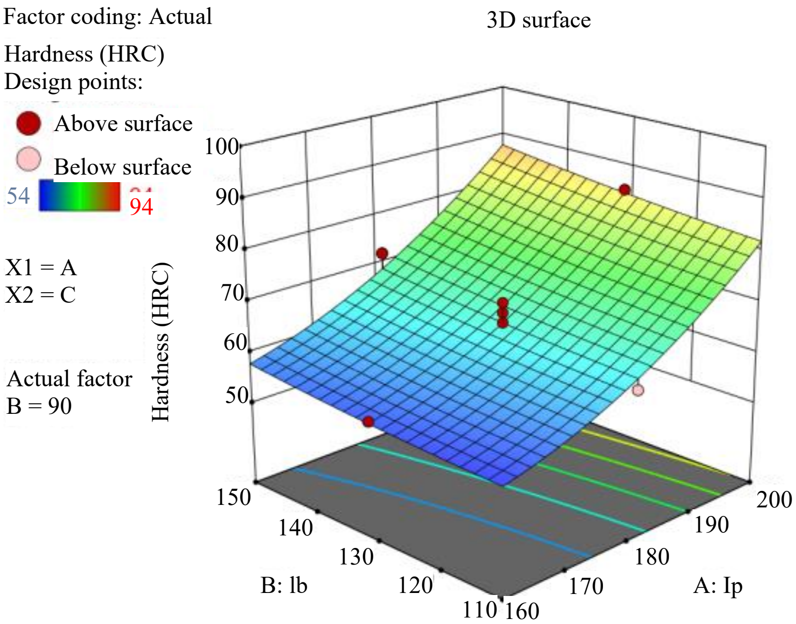

Figure 2. 3D surface plot of peak current and pulses per second for hardness.

The correlation between the peak current and tensile strength was remarkable, indicating a substantial influence. The tensile strength of the material was strongly affected by variations in the peak current, as evidenced by the 3D surface plot shown in Figure 4. The graph clearly illustrates that an increase in the peak current results in an increase in the tensile strength, whereas changes in the pulses per second have a comparatively lesser impact. The tensile strength increases with the peak current levels.

Model Fitting

In regression analysis, model fitting refers to the process of estimating the parameters of the regression model based on the available data. The objective was to identify the most suitable model that effectively represents the relationship between the dependent and independent variables, ensuring a good fit for the data. The regression equations for both output responses are as follows:

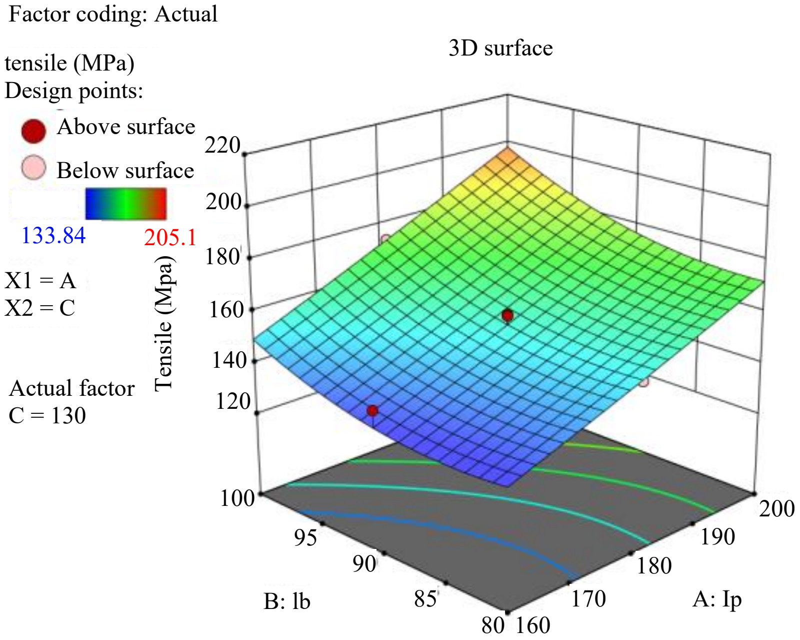

Figure 3. 3D surface plot of peak current and base current for tensile.

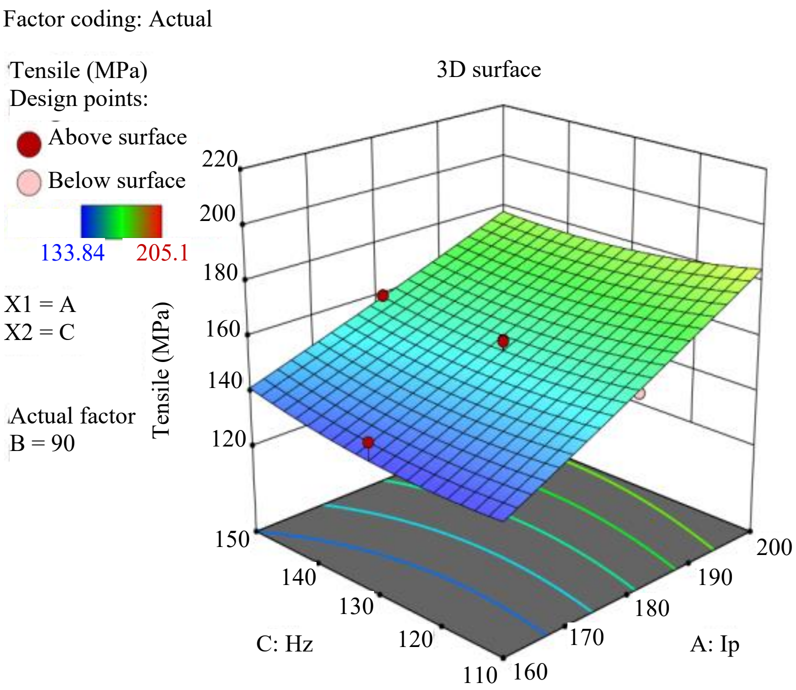

Figure 4. 3D surface plot of peak current and pulses per second for tensile.

Regression Equation of Hardness

Hardness = 509.35 + (-4.03938 × peak current) + (-3.19125 × base current) + (-0.435 × pulse per second) + (0.010625 × peak current × base current) + (0.0015625 × peak current × pulse per second) + (-0.000625 × base current × pulse per second) + (0.01 × peak current^2 + 0.01 × base current^2 + 0.00125 × pulse per second^2)

The equation expressed in terms of actual factors can be used to predict the reaction at particular levels of each element. In this instance, the levels of each element should be expressed in their original units.

Regression Equation of Tensile Strength

Tensile strength = (857.684) + (0.687772 × peak current) + (-16.6951 * Base current) + (-2.47867 * Pulse per second) + (0.0119313 × peak current × base current) + (-0.00897187 * Peak current × pulse per second) + (0.0187563 × base current × pulse per second) + (0.00140114 × peak current^2) + (0.0732045 × base current^2) + (0.00931364 × pulse per second^2)

This equation should not be used to determine the relative influence of each factor because the intercept is not at the center of the design space, and the coefficients are scaled to suit the units of each element.

Model Analysis

In RSM, model analysis involves the evaluation of the fitted model to assess its precision and reliability in predicting the response variable. The primary goal of the model analysis was to examine the performance of the fitted model and identify any influential factors or interactions that impact the response variable.

ANOVA for Hardness (WZ)

The ANOVA for hardness (WZ) is shown in Table 5.

The lack of fit F-value of 0.57 indicates that the lack of fit is not significant when compared to the pure error. There is a 72.19% chance that noise is the cause of the large lack of fit F-value. A non-significant lack of fit is ideal for the model.

ANOVA for Tensile Strength

The ANOVA for tensile strength is shown in Table 6.

The model appeared to be significant based on its F-value of 26.81. An F-value this high has a 0.01% chance of being the result of noise.

Table 5. ANOVA for hardness (WZ).

Source	Sum of squares	Df	Mean square	F-value	p-value
Model	2484.72	9	276.08	42.46	< 0.0001
A-Ip	2073.60	1	2073.60	318.89	< 0.0001
B-Ib	193.60	1	193.60	29.77	0.0003
C-Hz	52.90	1	52.90	8.14	0.0172
AB	36.12	1	36.12	5.56	0.0402
AC	3.12	1	3.12	0.4806	0.5039
BC	0.1250	1	0.1250	0.0192	0.8925
A^2	44.00	1	44.00	6.77	0.0264
B^2	2.75	1	2.75	0.4229	0.5301
C^2	0.6875	1	0.6875	0.1057	0.7518
Residual	65.02	10	6.50		
Lack of Fit	23.69	5	4.74	0.5732	0.7219
Pure Error	41.33	5	8.27		
Cor total	2549.75	19			
Fit summary					
Model degree	Quadratic–significant				
R^2	0.9745				
Adjusted R^2	0.9515				
Predicted R^2	0.9095				

ISSN: 2231-3818 (Online), ISSN: 2321-4236 (Print)

When the P-value is less than 0.0500, the model terms are deemed significant. In this case, A, B, and B2 are the significant model terms. If the values exceed 0.1000, the model terms are unimportant. If your model has many superfluous terms (aside from those required to maintain the hierarchy), model reduction may improve it.

The lack of fit F-value of 0.88 indicates that the lack of fit is not significant when compared to the pure error. There is a 55.41% chance that noise is the cause of the large lack of fit F-value. It is preferable to have a non-significant lack of fit.

Optimize Parameter

It involves creating a mathematical model that represents the relationship between the process variables and desired response. Table 7 lists the constraints of the goal, lower limit, and upper limit for the optimization.

Table 6. ANOVA for tensile strength.

Source	Sum of squares	Df	Mean square	F-value	p-value
Model	6778.78	9	753.20	26.81	< 0.0001
A-Ip	4836.92	1	4836.92	172.16	< 0.0001
B-Ib	1139.98	1	1139.98	40.58	< 0.0001
C-Hz	1.02	1	1.02	0.0364	0.8524
AB	45.55	1	45.55	1.62	0.2317
AC	103.03	1	103.03	3.67	0.0845
BC	112.58	1	112.58	4.01	0.0732
A^2	0.8638	1	0.8638	0.0307	0.8643
B^2	147.37	1	147.37	5.25	0.0450
C^2	38.17	1	38.17	1.36	0.2708
Residual	280.95	10	28.10		
Lack of Fit	131.50	5	26.30	0.8798	0.5541
Pure Error	149.46	5	29.89		
Cor total	7059.73	19			
Fit summary					
Model degree	Quadratic–significant				
R^2	0.9602				
Adjusted R^2	0.9244				
Predicted R^2	0.8056				

Table 7. Constraints in optimization.

Name	Goal	Lower limit	Upper limit
Input parameters			
A: Peak current (Amps)	is in range	160	200
B: Base current (Amps)	is in the range	80	100
C: Pulses per second (Hz)	is in range	110	150
Output parameters (Responses)			
Tensile (MPa)	Maximize	133.84	205.1
Hardness (HRC)	Maximize	54	94

Table 8. Suggested optimized solution.

Input variables	Suggested results at optimum condition	Output variables	Suggested results at optimum condition
Peak current (Amps)	200	Tensile strength (MPa)	202.393
Base current (Amps)	100	Hardness (HRC)	95.252
Pulse per second (Hz)	150		
Desirability: 0.981			

Table 9. Confirmation test results.

<table>
<tr><th colspan="7">Input process parameters at optimum conditions</th></tr>
<tr><td colspan="2">Peak current: 200 Amp</td><td colspan="3">Base current: 100 Amp</td><td colspan="2">Pulse per second: 150 Hz</td></tr>
<tr><th colspan="7">Experimental results—output parameters</th></tr>
<tr><td rowspan="2">Tensile strength</td><td>Width (mm)</td><td>Thickness (mm)</td><td>Area (mm^2)</td><td>Load (N)</td><td>Tensile strength (MPa)</td><td>Avg. tensile strength (MPa)</td></tr>
<tr><td>13</td><td>8</td><td>104</td><td>21330</td><td>205.100</td><td>205.100</td></tr>
<tr><td rowspan="3">Hardness</td><th colspan="5">Hardness at weld zone (WZ)</th><th rowspan="2">Avg. hardness (WZ)</th></tr>
<tr><td colspan="2">Top</td><td>Center</td><td colspan="2">Bottom</td></tr>
<tr><td colspan="2">91</td><td>96</td><td colspan="2">95</td><td>94</td></tr>
</table>

Table 10. Comparison of predicted results with experimental results.

Parameters		Predicted results at optimum conditions	Experimental results	% of deviation
Input	Peak current (Amps)	200	200	--
	Base current (Amps)	100	100	--
	Pulse per second (Hz)	150	150	--
Output	Tensile strength (MPa)	202.393	205.100	1.33
	WZ Hardness (HRC)	95.252	94.000	1.31

The suggested optimized solutions, which are provided by Design-Expert software for the output responses, are listed in Table 8.

VALIDATION OF RESULTS

Validating the results derived from the RSM is an essential and crucial stage for guaranteeing the precision and dependability of the optimization procedure. Validation involves assessing the model quality and determining its capacity to accurately predict the response variable across various scenarios.

A confirmation test was performed to validate the output responses. This test was carried out based on the suggested parameters provided by the Design-Expert software. Table 9 displays the results of the confirmation test, which was conducted to validate the findings.

After performing the confirmation test, it needs to be compared with the predicted results provided by the software and the percentage of deviation. The required values are under 5% for the validation of results, as mentioned in Table 10.

It is clearly observed that the tensile strength and hardness are within the acceptable range, which means that these parameters are below 5%, which is desirable.

CONCLUSIONS

In the current study, the focus is on analyzing the hardness and tensile strength of the weldment formed by the PC-TIG welding process for an 8 mm thick plate of composite aluminum alloy weld joint of AA5052 and AA6063. Through the examination of results and discussions, the study draws the following conclusions regarding the observed outcomes and findings:

1. The peak current, base current, and pulses per second were the most significant parameters for hardness and tensile strength.
2. From the analysis and experimental results, it was concluded that the maximum result was achieved at a peak current of 200 A, base current of 100 A, and pulses per second of 150 Hz.
3. The maximum hardness value was 94 HRC when the peak current was 200 A, base current was 100 A, and pulse per second was 150 Hz.
4. The tensile strength was good at 205.10 MPa when the peak current was 200 A, the base current was 100 A, and pulses per second was 150 Hz.
5. The tensile strength and hardness increased as the peak current, base current, and pulses per second increased.
6. The optimized parameters were a peak current of 200 A, a base current of 100 A, and a pulse per second 150 Hz. provides a mechanically sound and defect-free weld.
7. From all experiments, it is clear that for better results and welding quality, the welding current is highly effective for good penetration.

This study highlights that composite aluminum alloys, such as AA5052 and AA6063, demonstrate improved weld quality with increasing peak current, base current, and pulses per second, leading to enhanced mechanical soundness and defect-free joints. Optimizing these parameters is crucial for achieving superior hardness, tensile strength, and penetration, making these alloys highly suitable for advanced welding applications.

Acknowledgement

The authors express their gratitude to the management of Atmiya University, Rajkot, for their support and permission to utilize the welding facility and other necessary resources of the university.

Declaration of Competing Interest

There is no competing interest.

REFERENCES

1. Mathers G. The Welding of Aluminium and Its Alloys. Cambridge: Woodhead Publishing; 2002. doi:10.1533/9781855737631.
2. Kevorkijan VM. Aluminum composites for automotive applications: a global perspective. JOM. 1999;51(11):54-58. doi:10.1007/s11837-999-0224-2.
3. Kumar A, Milton MS. A comparison of welding techniques of aluminium alloys: a literature review. Int J Sci Res Sci Eng Technol. 2016;2:172-175.
4. Reddy GM, Gokhale AA, Rao KP. Optimisation of pulse frequency in pulsed current gas tungsten arc welding of aluminium-lithium alloy sheets. Mater Sci Technol. 1998;14(1):61-66. doi:10.1179/mst.1998.14.1.61.
5. Hori K, Watanabe H, Myoga T, Kusano K. Development of hot wire TIG welding methods using pulsed current to heat filler wire: research on pulse heated hot wire TIG welding processes. Weld Int. 2004;18(6):456-468. doi:10.1533/wint.2004.3281.
6. Shrivas SP, Vaidya SK, Khandelwal AK, Vishvakarma AK. Investigation of TIG welding parameters to improve strength. Mater Today Proc. 2020;26:1897-1902. doi:10.1016/j.matpr. 2020.02.416.
7. Parthasarathy C, Sathyaseelan D. An investigation on effect of process parameter of pulsed TIG welded aluminum alloy on mechanical and corrosion properties. Int J Res Appl Sci Eng Technol. 2015;3(10):437-441.
8. Kumar BA, Raveendra A. Effect of pulsed and non-pulsed current on welding characteristics of AA6061 aluminium alloy welded joints using TIG welding. Int J Eng Res Sci. 2016;2:93-102.

9. Hasanniah A, Movahedi M. Welding of Al-Mg aluminum alloy to aluminum clad steel sheet using pulsed gas tungsten arc process. J Manuf Process. 2018;31:494-501. doi:10.1016/j.jmapro.2017.12.008.
10. Yelamasetti B, Vardhan VR, T VV. Weldability and mechanical properties of AA5052 and AA7075 dissimilar joints developed by GTAW process. Mater Today Proc. 2021;47:4162-4166. doi:10.1016/j.matpr.2021.04.446.
11. Yelamasetti B, Ramana GV, Vardhan TV. Optimization of GTAW parameters for the development of dissimilar AA5052 and AA6061 joints. Mater Today Proc. 2021;47(Pt 14):4350-6. doi:10.1016/j.matpr.2021.04.633.
12. Eazhil KM, Mahendran S, Kumar SG. Optimization of tungsten inert gas welding on 6063 aluminum alloy on Taguchi method. Int J Res Sci Innov. 2014 Aug;1(3):1-5.
13. Kumar A, Sundarrajan S. Optimization of pulsed TIG welding process parameters on mechanical properties of AA5456 aluminum alloy weldments. Mater Des. 2009;30(4):1288-1297. doi:10.1016/j.matdes.2008.06.055.
14. Shunmugasundaram M, Praveen Kumar A, Ponraj Sankar L, Sivasankar S. Optimization of process parameters of friction stir welded dissimilar AA6063 and AA5052 aluminum alloys by Taguchi technique. Mater Today Proc. 2020;27:871-876. doi:10.1016/j.matpr.2020.01.122.
15. Montgomery DC. Design and Analysis of Experiments. New York: John Wiley & Sons; 2017.
16. Honu E, Guo S, Rahman S, Zeng C, Mensah P. Advancing hydrogen gas utilization in industrial boilers: impacts on critical boiler components, mitigation measures, and future perspectives. Hydrogen. 2024;5(3):574-623. doi:10.3390/hydrogen5030032.
17. Yadav GPK, Bandhu D, Krishna BV, Gupta N, Jha P, Vora JJ, et al. Exploring the potential of metal-cored filler wire in gas metal arc welding for ASME SA387-Gr.11-Cl.2 steel joints. J Adhes Sci Technol. 2024;38:163-184. doi:10.1080/01694243.2023.2223367.
18. Meyer RM, Suffield SR, Hirt EH, Suter JD, Lareau JP, Zhuge JW, Qiao H, Moran TL, Ramuhalli P. Nondestructive examination guidance for dry storage casks. Richland (WA): Pacific Northwest National Laboratory; 2016. Report No.: PNNL-24412 Rev. 1. doi:10.2172/1333454.
19. Polzin T, Schwenk D. World-wide unified scales for the Rockwell hardness test: results of the round robin test and differences between the laboratories. Mater Test. 2000;42:460-467. doi:10.1515/mt-2000-4211-1211.
20. Anderson VL, McLean RA. Design of Experiments: A Realistic Approach. Boca Raton, Florida, United States: CRC Press; 2018. doi:10.1201/9781315141039.

